

# Three-Dimensional Ballistocardiography and Respiratory Motion in Sustained Microgravity

G. K. PRISK, PH.D., S. VERHAEGHE, M.D., D. PADEKEN, DR.ING., H. HAMACHER, DR.ING., AND M. PAIVA, PH.D.

PRISK GK, VERHAEGHE S, PADEKEN D, HAMACHER H, PAIVA M. *Three-dimensional ballistocardiography and respiratory motion in sustained microgravity*. *Aviat Space Environ Med* 2001; 72:1067-74.

**Background:** We measured the three-dimensional ballistocardiogram (BCG) in a free-floating subject in sustained microgravity during spaceflight to test the usefulness of such measurements for future non-invasive monitoring of cardiac function, and to examine the effects of respiratory movement on the BCG in three axes. **Methods:** Acceleration was measured using a three-axis accelerometer fastened to the lumbar region of the subject while simultaneous recordings of ECG, and respiratory motion via impedance plethysmography were also made. Data were recorded during a 146-s period of inactivity on the part of the subject during which time there was no contact with the spacecraft. **Results:** Total body motion due to respiratory activity was consistent with that calculated from the known action of the diaphragm and conservation of momentum. The accelerations due to cardiac activity, ensemble averaged over the R-R interval, were greatest along the head-to-foot axis. Maximum amplitude of the HIJK complex of the BCG generated by ventricular ejection was greatest in the head to foot axis ( $\sim 70 \cdot 10^{-3} \text{ m} \cdot \text{s}^{-2}$ ), but there were also substantial accelerations along the dorso-ventral axis of up to  $43 \cdot 10^{-3} \text{ m} \cdot \text{s}^{-2}$ , that are not measured in terrestrial two-dimensional studies. The amplitude of the BCG was strongly affected by lung volume, with accelerations being reduced 50 to 70% between end-inspiration and end-expiration. **Conclusions:** These data suggest a greatly reduced transmission of the cardiac motion to the body at end-expiration (FRC) than at higher lung volumes. The BCG might be further developed as a non-invasive means of monitoring parameters such as stroke volume in microgravity.

**Keywords:** microgravity, weightlessness, 3-D ballistocardiography, respiratory motion.

THE BALLISTOCARDIOGRAM (BCG) is the movement of the entire body resulting from the action of the beating heart within it. Gordon made the first published recordings of the BCG in 1877 using a spring weighing machine (15). Over the years, recordings were made using various techniques, including attempts to measure cardiac stroke volume (2). Despite extensive work on the development of the BCG, the technical limitations encountered were too great for routine use, and the technique has never found favor.

The BCG is difficult to measure on the ground, since the subject must be de-coupled from the environment in order to measure the motion, or such motion must be inferred, using for example a static charge-sensitive bed (8,11). However, in microgravity, subjects can be free-floating, enabling simpler techniques. In addition, because the BCG is a passive recording technique, it may be well-suited to continuous monitoring of cardiac function in microgravity, such as during sleep. When

augmented with other more direct measures of cardiac stroke volume (e.g., echocardiography or soluble gas rebreathing), BCG may become a useful monitoring tool.

Because gravity always constrains movement in two axes, three-dimensional (3-D) BCG is not feasible in terrestrial laboratories. Three-dimensional BCG has been inferred from tri-axial force measurements on the ground (15), but direct measurement of the acceleration of the body in all three axes is not possible. There have, however, been some studies performed in microgravity. Hixson et al. (6) measured the BCG on apneic subjects restrained in a rigid frame during short periods ( $\sim 25$  s) of weightlessness during parabolic flights. In 1982, a Russian study reported the results of ballistocardiographic examinations on the Salyut-6 spaceflight (1). They recorded the acceleration only in the head to foot direction, and noted an increase in systolic wave amplitude during a breathhold at end-inspiration late in flight. In 1983, during the Spacelab flight D-1, Scano et al. (13) found an increase in the amplitude of the BCG in the dorso-ventral axis compared with that of subjects suspended in 1 G, but experimental difficulties precluded measurements in other axes. These are the only cases we are aware of where 3-D ballistocardiography has been performed.

During the Spacelab flight D-2 in 1993, an opportunity became available to perform a feasibility study in which we recorded the 3-D BCG on a free-floating subject breathing normally. Instrumentation on board provided us with high sensitivity three-axis accelerometers and the ability to record ECG and respiration non-invasively. The results presented here are the out-

From the Department of Medicine, University of California San Diego, La Jolla CA (G. K. Prisk); Biomedical Physics Laboratory, Universite Libre de Bruxelles, Brussels, Belgium (S. Verhaeghe, M. Paiva); Institute für Luft-und Raumfahrtmedizin, Cologne, Germany (D. Padeken); and Institute für Raumsimulation, Cologne, Germany (H. Hamacher).

This manuscript was received for review in October 2000. It was revised in April 2001. It was accepted for publication in July 2001.

Address reprint requests to: G. Kim Prisk, Ph.D., who is Professor of Medicine, Department of Medicine, 0931, University of California, San Diego, 9500 Gilman Dr., La Jolla, CA 92093-0931; kprisk@ucsd.edu.

Reprint & Copyright © by Aerospace Medical Association, Alexandria, VA.

come of that opportunity. We wished to determine the feasibility of making high-quality measurements of the BCG in microgravity. In addition, because we could simultaneously measure respiratory motion, we could examine the effects of changes in lung volume on the BCG under virtually ideal conditions, and calculate the motion of the body due to respiratory motion. We reasoned that such a pilot study would lay the groundwork for future use of the BCG in the microgravity environment, such as in the non-invasive monitoring of changes in cardiac stroke volume.

## METHODS

### *Subjects and Data Recording*

We recorded the BCG along three orthogonal axes, the respiratory movements of the ribcage and the abdomen, as well as the electrocardiogram (ECG), in one subject in sustained microgravity, over a period of 15 min. The subject, a crewmember of the D-2 Spacelab mission which flew in 1993, was a 42-yr-old male with a preflight weight of 81 kg, and height of 179 cm. The measurement was made after 8 d in orbit by which time cardiac output, measured by acetylene rebreathing within 1 d of this study, was  $6.2 \text{ L} \cdot \text{min}^{-1}$  (less than 5% above 1 G upright control values) and stroke volume was 88 ml (elevated by 14% above 1 G upright control values) (16). Because of the nature of the study (an experiment of opportunity), no ground control measurements of the BCG were feasible. The protocol was approved by the IRB of the German Space Agency, and the subject gave informed consent.

A triaxial accelerometer (MMA, ERNO Raumfahrt-technik/Deutsche Aerospace, Bremen, Germany; absolute measurement range:  $3 \cdot 10^{-6} \text{ g}$  to  $100 \cdot 10^{-3} \text{ g}$ ; frequency measurement range: 0.1 to 100 Hz; dimensions: 33 mm x 87 mm x 63 mm; mass: 165 g) was tightly taped in the lumbar region of the subject so that motions of the accelerometer were those of the subject's body. This was linked to the recording computer with a light umbilical cord and data were sampled at 300 Hz.

Respiratory motion was measured using a respiratory inductive plethysmography (RIP) with coils around the ribcage and the abdomen sewn into a close fitting Lycra Spandex suit (17). ECG was recorded from a three-lead system. RIP data were recorded at 100 Hz and ECG at 500 Hz. These signals were fed to the recording computer by a separate umbilical to that used for the accelerometer data. The two flexible umbilicals formed the only mechanical connection between the Spacelab structure and the subject who was asked to float, relax and breathe normally. Examination of the video record showed that the umbilical cables were never taught during the period of the recording.

### *Axis System*

We chose to use the nomenclature for the axes that is the standard in ballistocardiography (14), where Y is the longitudinal body axis (positive to the head), X is the lateral axis (positive to the right) and Z is the ventro-dorsal axis (positive to the back) (Fig. 1). Note

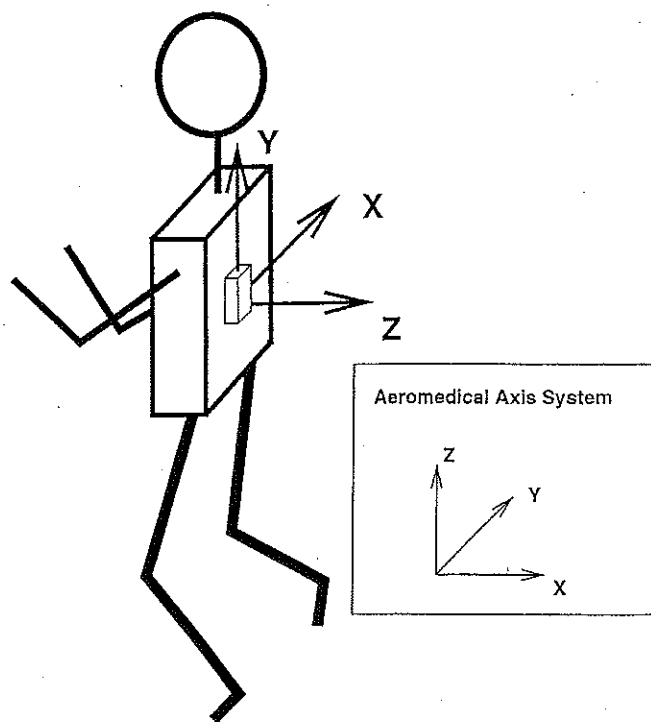


**Fig. 1.** Conventions for ballistocardiographic spatial axes. The arrows point in the positive direction. Y is the longitudinal body axis (positive to the head), X is the lateral axis (positive to the right) and Z is the ventro-dorsal axis (positive to the back). This nomenclature is the standard in ballistocardiography. The inset shows the conventional aeromedical axis system in common use.

that this nomenclature is different from the conventional aero-medical axis system.

### *Analysis of the BCG*

We selected the longest uninterrupted period of the recording during which no contact with the Spacelab structure or with the other astronauts occurred (verified from a video recording), a continuous 146 s period. All the BCG data reported are from this period.

Data (ECG, BCG and RIP) were first resampled at the lowest common multiple frequency 1500 Hz, using a lowpass interpolation algorithm (7). Then, R waves of the ECG were identified by threshold detection on the signal and its derivative. Detected R waves were used as reference points to identify the cardiac cycle length. For each cardiac cycle, the ECG and BCG were represented against a normalized time axis: the beginning of each cycle was set to 0% and the end to 100%. Normalized curves of the ECG and BCG were superimposed to compute average BCG and ECG signal in the normalized cardiac cycle (ensemble averaging). The resultant average BCG had an associated SD of  $\sim 2 \cdot 10^{-3} \text{ m} \cdot \text{s}^{-2}$  in all three axes. Normalizing to the R-R interval, gave better reproducibility of the superimposed ECG and BCG curves than simply aligning each beat at the beginning of the R wave since there was some variation in the R-R interval.

We averaged the BCG in four distinct conditions related to the respiratory phase. These phases were that near Functional Residual Capacity (FRC) defined as the interval from 500 ms before the minimum volume ex-

cursion to 66 ms after. Similarly, the volume near FRC + tidal volume ( $FRC + V_T$ ) was defined as the interval from 500 ms before the minimum volume excursion to 66 ms after. These ranges were found to be the best compromise between having as many beats as possible in a respiratory interval, and having a well-defined respiratory interval. Fig. 2 shows the changes in BCG between FRC and  $FRC + V_T$ . The other two phases selected the BCG close to the middle of inspiration and to the middle of expiration (Fig. 3). In these cases, the interval of BCG selection was 500 ms before and after the mid-point of the volume excursion. Velocity and displacement were computed by integrating the ensemble-averaged acceleration signals once or twice with respect to time along each axis.

*Significant Points on the BCG*

In order to characterize the curves, a lettering nomenclature similar to that used for the ECG was applied to the head to foot accelerations (Fig. 2). According to Dock et al. (2) the initial headward impulse, H, was ascribed to the initial isovolumetric ventricular contraction, the initial footward impulse, I, to the ventricular recoil from ejection, and the main headward wave, J, was ascribed to the impact of the ejected blood on the

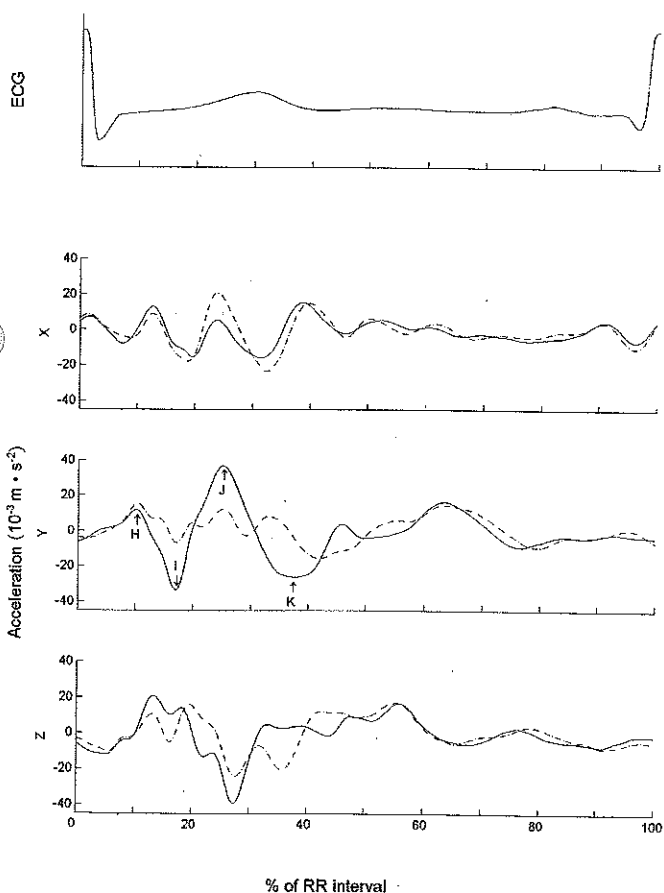


Fig. 2. Average tracing of ECG and BCG at different lung volumes. The dashed curves show the mean BCG measured close to the Functional Residual Capacity (average of 31 beats) and the solid curves represent the mean BCG measured close to Functional Residual Capacity + Tidal Volume (average of 40 beats). The abscissa is the R-R interval expressed as a percentage.

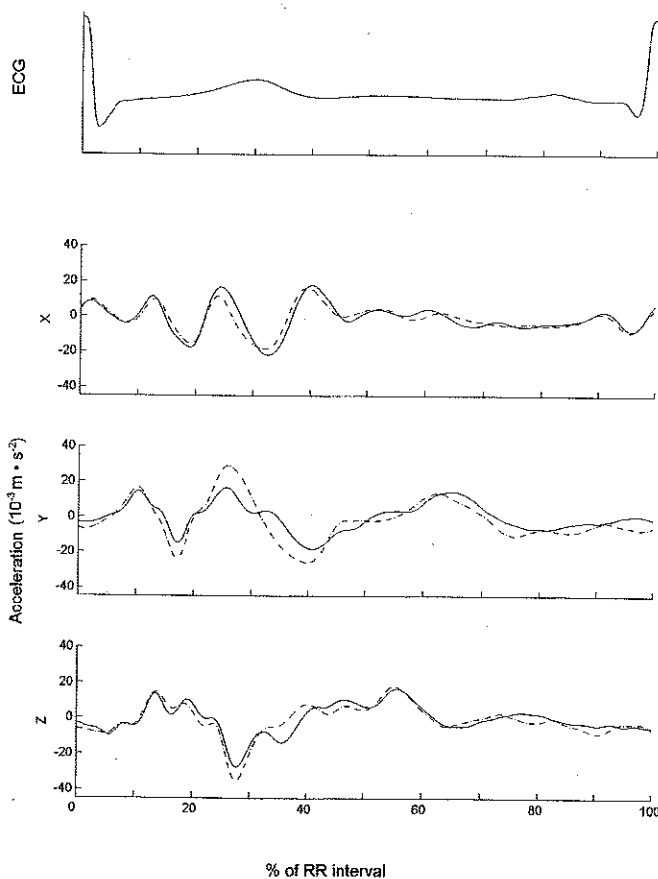


Fig. 3. Average tracing of ECG and BCG measured at mid-inspiration (average of 33 beats, dashed line) and mid-expiration (average of 30 beats, solid line). Figure format as Fig. 2.

aortic arch. The K wave was thought to be due to deceleration of blood flowing footward in the aorta (2). We utilized this classic nomenclature in describing the events in our 3-D BCG.

*Respiratory Motion*

Respiratory motion was recorded at the same time as the acceleration allowing us to analyze the effects of respiratory action on the displacement of the entire body. We used the same data set as that used for the analysis of the BCG. The beginning and end of each respiratory cycle were identified in the signals from the RIP. Data from each of the 43 respiratory cycles were then normalized to a scale of 0 to 100% in a manner analogous to that used for the ECG. Acceleration data from each cycle were then ensemble averaged to produce the average acceleration in each axis over the respiratory cycle. These accelerations were then integrated once to give the velocity, and twice to give the displacement of the body resulting from respiratory motion. The effect of ensemble averaging over the length of the respiratory cycle is to average out the motion due to the action of the heart, since the position of the heart beats within the multiple cycles is random with respect to the beginning of the breath.

*Reproducibility*

During the 15 min of the experiment, several shorter records of stable data, as well as the 146-s sample pre-

TABLE I. BCG ACCELERATIONS.

Axis	Experimental Conditions	Lung Volume	BCG phase		
			HI	IJ	JK
X	3-D this study	FRC	-23	+33	+31
		FRC + V <sub>T</sub>	-29	+22	+31
	3-D Parabolic flight (6)	% Change	-21%	+50%	0%
		Apnea	-43	+50	+23
Y	3-D this study	FRC	-19	+16	-19
		FRC + V <sub>T</sub>	-44	+70	-63
	3-D Parabolic flight (6)	% Change	-57%	-77%	-70%
		Apnea	-23	+30	-23
	2-D Ground (2)	Deep-insp	-42	+59	-39
		% Change	-20%	-37%	-34%
Z	3-D this study	FRC	-13	+17	+26
		FRC + V <sub>T</sub>	-10	+4	+43
	3-D Parabolic flight (6)	% Change	+30%	+325%	-40%
		Apnea	-28	+30	+18

Axes X, Y and Z are the orthogonal axes shown in Fig. 1.

BCG Phase refers to the peak-to-peak amplitude within the HIJK complex. (See Fig. 2 and text for details).

Acceleration data are in  $10^{-3} \text{ m} \cdot \text{s}^{-2}$ .

Experimental conditions: 3D this study—data collected in sustained microgravity. 3D Parabolic Flight—data collected by Hixson et al. (6) during parabolic flight. 2D Ground—data (2) collected in a terrestrial setting.

Lung Volume: The lung volume at which the measurement was taken: FRC and FRC + V<sub>T</sub>—during sustained microgravity (see text for details). Apnea—Not defined but assumed to be a lung volume above FRC (6). Deep-insp—Not defined but above FRC (2).

% Change: The percentage change in the waveform amplitude indicated from the high lung volume condition to the low lung volume condition. For the data from this study this refers to the change from FRC + V<sub>T</sub> to FRC. For the 2D Ground data this refers to the change from a "deep inspiration" to a "deep expiration" (latter data not shown; see ref. 2).

sented in this paper, were also tested to see if the patterns of these periods are similar to this sample. These other periods lasted between 10 and 40 s. We did not find significant differences of the amplitudes of the curves for these different segments of data during the experiment.

## RESULTS

### Cardiac Motion

In Fig. 2, the acceleration in each of the three axes shows two different curves: the broken line represents the acceleration near the end of expiration (FRC), and the solid line that near the end of inspiration (FRC + V<sub>T</sub>). The H, I, J and K waves are the largest waves of the BCG and are marked. Table I gives the values of the maximum peak to peak accelerations generated between these events, in three different axes of recording during spaceflight. For the purposes of comparison, Table I also lists the peak-to-peak amplitudes of these waves recorded during a breathhold in parabolic flight by Hixson et al. (6). In addition, typical amplitudes of the acceleration in the longitudinal body axis (Y) reported during a post-inspiratory breathhold in a terrestrial laboratory are shown (2).

Overall there was large reduction in the BCG amplitude at end-expiration (the average of 31 beats) compared with end-inspiration (40 beats, Fig. 2, Table I). While the traditionally defined HIJK complex is clearly visible at FRC + V<sub>T</sub>, it is unclear and poorly defined at FRC.

In the traditionally used longitudinal body axis (Y), the entire pattern at FRC is of lower amplitude than that

at FRC + V<sub>T</sub>, and particularly the IJ wave where there is a 77% reduction (see Table I). It appears that at FRC, the large J wave has split up into three smaller waves (see Y axis data on Fig. 2). The other peaks also show a substantial reduction in amplitude at FRC compared with FRC + V<sub>T</sub>.

In the X-axis (transverse), the IJ wave is the only significant wave where the amplitude is greater at FRC ( $+33 \cdot 10^{-3} \text{ m} \cdot \text{s}^{-2}$ ) than FRC + V<sub>T</sub> ( $+22 \cdot 10^{-3} \text{ m} \cdot \text{s}^{-2}$ ), a 50% increase (see Table I). The other waves on the two curves along this axis are similar (see X axis data on Fig. 2 and Table I).

In the Z-axis (dorso-ventral), the shape of the pattern during the systolic phase at FRC is different than that at FRC + V<sub>T</sub> (see Z axis data on Fig. 2). The peak to peak IJ wave is smaller at FRC + V<sub>T</sub> than at FRC with a 76% reduction, and during the J wave, several events along this axis are visible.

Fig. 3 shows the BCG at the middle of inspiration (33 beats, broken line) and the middle of expiration (30 beats, solid line). The differences in acceleration between mid-inspiration and mid-expiration are much smaller than the differences seen between FRC + V<sub>T</sub> and FRC (compare Fig. 3 and Fig. 2). There are only minor differences between the BCG at a similar lung volumes, regardless of the direction of respiratory motion. In the Y-axis, the IJ wave at the middle of inspiration is similar in shape to the curve at FRC + V<sub>T</sub>, while at the middle of expiration the curve shape is similar in shape to that at FRC, suggesting a strong influence of pleural pressure.

Integration of the acceleration (Fig. 2) twice with respect to the time gives the free trajectory of the center

of mass of the subject (Fig. 4). The format of the figure is the same as that for Fig. 2 with the broken line representing the displacement at the FRC, and the solid line at FRC +  $V_T$ . For the latter, and along the Y-axis, the displacements corresponding to the IJ and JK waves identified in Fig. 2 are  $-35 \mu\text{m}$  and  $+89 \mu\text{m}$ , respectively.

On the videotape recorded during the experiment, it could be seen that the subject drifted from his initial point at the beginning of the free float period. This drift was the consequence of several uncontrollable factors: the airflow in the Spacelab, prior contact between the astronaut and the wall of the Spacelab, the movements of the subject as well as any potential physiological drift. In this analysis, we eliminated any drift from the data, by forcing to zero the displacement of the body after each cardiac cycle.

*Respiratory Motion*

Fig. 5 shows the velocity and displacement of the body resulting from the effects of respiratory motion. Because the data are averaged over many non-aligned cardiac cycles, the BCG averages out and cannot be seen. The upper panel shows the averaged signal from the RIP system for the 43 breaths present in the data set. Inspiration accounted for approximately 40% of the total time of the respiratory cycle. The lower three

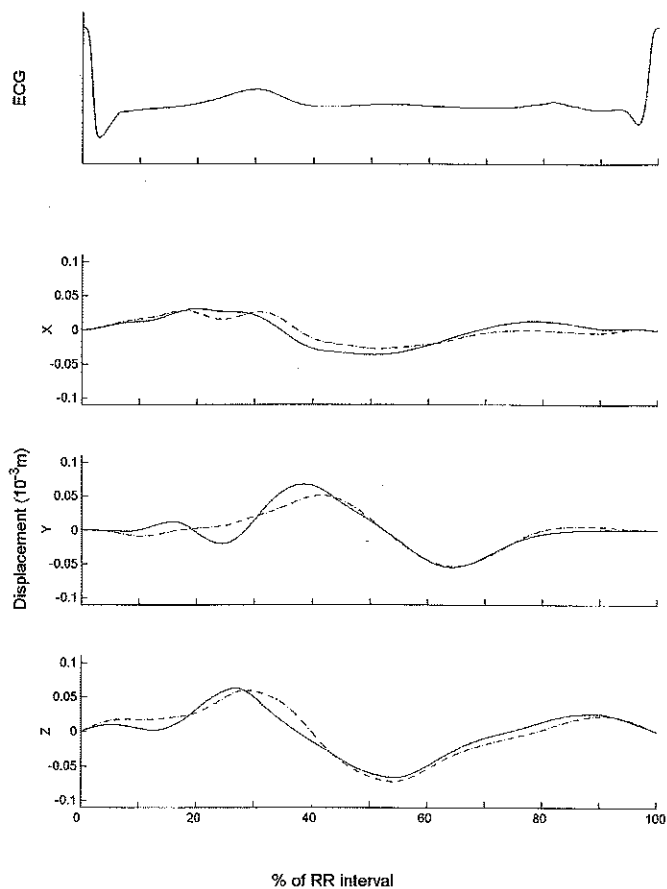


**Fig. 4.** Average tracing of ECG and displacement of the center of mass of the subject measured at FRC (dashed line) and at FRC +  $V_T$  (solid line). Peak to peak displacements between the positions of the IJ and JK waves as defined in Fig. 2 were calculated. Figure format as Fig. 2.

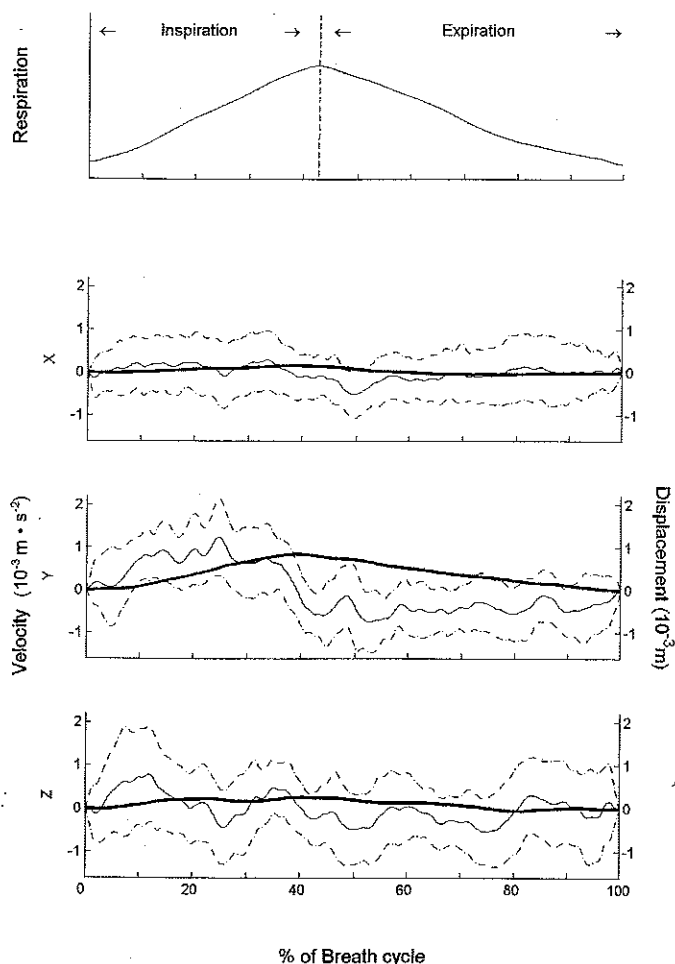


**Fig. 5.** Respiration is the average tracing of lung volume measured from the respiratory inductive plethysmograph (top), velocity (fine line)  $\pm$  SD, and displacement (heavy line) averaged over 43 respiratory cycles. The portions of the respiratory cycle corresponding to inspiration and expiration are shown. See text for details.

panels show the velocity  $\pm$  SD and the displacement of the subject's body resulting from respiratory motion in the X (lateral), Y (head to foot), and Z (dorso-ventral) axes. The greatest velocity was seen in the Y-axis with an initial headward value of  $1.2 \text{ mm} \cdot \text{s}^{-1}$ . This resulted in an overall headward displacement of the body of 0.9 mm. Motions in the other axes were much smaller.

**DISCUSSION**

Ballistocardiography is a non-invasive technique that measures the movements of the body and uses the results to infer information about the mechanical activity of the heart (2). Even if the events within the heart were as simple as the ejection of a bullet from a cartridge, the events and forces acting on the body are complex. For example, the motion of the body comes from breathing as well as from the heartbeat; and the coupling of the heart to the body is also complex. In this study we recorded the 3-D BCG of an unrestrained free-floating subject in microgravity. The data showed significant accelerations along the dorso-ventral axis, accelerations that are not measurable using conventional 2-D recording techniques in the terrestrial setting.

These accelerations are compatible with the known anatomical action of the heart in the body. In addition, we recorded respiration throughout the period of data collection allowing us to study the BCG at different phases of the respiratory cycle. These data show that the BCG is strongly modulated by lung volume with much higher accelerations recorded at higher lung volumes than at low lung volumes, but largely unaffected by the direction of the respiratory motion itself. The data we presented may serve a dual purpose: 1) to offer to those interested in the interpretation of ballistocardiograms a unique set of high quality data obtained in optimal conditions; 2) to open new applications in space, where new non-invasive techniques are required in the monitoring of the cardiorespiratory system of the astronauts. Ballistocardiography may prove useful in the setting of non-invasive monitoring of cardiac function during situations such as sleep and recovery from exercise.

The interpretation of a ballistocardiogram recorded on Earth has its qualitative and quantitative limitations. The most important of these limitations may be summarized as follows (3):

1) The BCG is not recorded in all degrees of freedom in a terrestrial laboratory. Three-dimensional force measurements (as opposed to measurements of acceleration) performed in 1 G have shown qualitatively similar results to those measured here (15). In microgravity the body can freely move in all directions.

2) The BCG is not caused solely by blood-mass-displacements. Other influences such as respiration are important to take into account.

3) In the terrestrial laboratory the BCG is dependent on the physical characteristics of the suspension system which is absent in these experiments performed in microgravity.

#### *Cardiac Motion*

The BCG pattern we recorded at FRC +  $V_T$  in the Y-axis closely matches the Y-axis acceleration pattern recorded with a 2-D BCG, and shows a clearly defined HIJK complex. The physiological interpretation of the principal forces responsible for the ballistocardiogram was only possible in two dimensions from terrestrial recordings. However, the BCG records measured in microgravity allow us to consider the contribution of the accelerations along the dorso-ventral axis (Z) in the understanding of the physiological forces appearing during a cardiac cycle. Some of these accelerations are substantial (Fig. 2).

Several forces combine to form the ballistocardiogram (BCG). One such force is the recoil of a chamber from which blood is being ejected, by muscular contraction as in the ventricle and atria. Another force is the relaxation of stretched elastin and collagen fibers, as in the atria in early diastole. Other sorts of forces are the impact of moving blood at a curve, or the motions of an elastic tube as a pressure wave moves along it (2).

The H wave results from the isovolumetric motion of the ventricle at the beginning of the onset of ventricular contraction, when the mitral leaflets close to form a septum which bulges into the atrium as pressure rises

(2). This forces the atrial contents to the right (+X), headward (+Y) and dorsally (+Z). In the present study, this wave is only clearly visible along the Y-axis, although there may be a small +X component (Fig. 2).

The I wave is thought to be due principally to recoil of the heart from systolic ejection. The recoil of the body associated with this is to the left (-X), footward (-Y) and ventrally (-Z). This is consistent with the 3-D BCG, where the I wave shows a ventral (negative) force along the Z-axis during the recoil of the heart, although this is small.

The J wave is the most prominent feature of normal tracing on a 2-D Table. This was also the case in our 3-D recording. The J wave is due to impact of the pulse wave on the aortic arch on the left side and on the bifurcation of the pulmonary artery on the right side (2). This force is rightward (+X), and headward (+Y). During the beginning of the ejection phase, along the Z-axis, the major force is predominately ventral, likely reflecting the geometry of the aortic arch.

The final wave (K) of the systolic complex, rightward (+X), footward (-Y) and dorsal (+Z), is due to the deceleration of blood flowing in the descending aorta. Fig. 2 shows that this wave is significant along the Y-axis, but small along the Z-axis. This is consistent with the anatomy of the descending aorta which is predominately longitudinal.

#### *Comparison with Previous Studies*

In their 3-D study of the BCG performed in short periods of microgravity, Hixson et al. (6) recorded the BCG during parabolic flight with the subject fastened on his back in a constraint platform to which the accelerometers were attached. All data were recorded with the subject apneic. Although there is no record of the actual lung volume during the breathhold, this appears to have been above FRC. The other studies performed in microgravity do not provide sufficient information to allow quantitative comparison with our data.

The data we obtained in an unrestrained, free-floating subject at FRC +  $V_T$ , closely resemble those of Hixson et al. (6) recorded in parabolic flight (Table I). The general shapes of the curves from these two different experiments are similar along the three axes. However, direct comparisons of the peak accelerations between our study on that of Hixson (6) are not possible because of the significant methodological differences between these two studies.

#### *Modification of the Ballistocardiogram with Respiratory Movements*

Normal breathing induces a respiratory variation in the BCG wave amplitude associated with intrathoracic pressure variation (2). The simultaneous record of BCG and respiration we recorded allows us to determine the importance of the role played by respiration on the BCG. Previous studies have shown that the size of the BCG wave amplitude may vary as much as 80% from the smallest at the end of expiration, to the largest at the end of inspiration (2). Our data confirm that.

The Y-axis acceleration in Fig. 2 shows a clear HIJK

complex at  $FRC + V_T$  which is very much smaller at FRC. There are several potential factors that likely contribute to these changes during the respiratory cycle (2).

1) The anatomical axis of the heart changes with lung volume. As the diaphragm rises in expiration, the heart and the ascending aorta become more transverse (2), reducing the Y-axis and increasing the X-axis IJ wave (Table I).

2) At FRC, the lung is more compliant than at higher lung volumes and so acts as a more efficient shock absorbing material, isolating the body from the motion of the heart. While this likely contributes, the fact that some accelerations actually increase at FRC, suggests that other factors are also important. Whether there is a difference in transmission properties between the heart and the body in microgravity compared with 1 G due to increased intrathoracic blood volume is unknown.

3) The contribution of the right heart may also be important. During inspiration, the decreasing intrathoracic pressure augments the return of blood to the right heart. A previous study (2) reported a mean decrease in Y-axis IJ amplitude of 37% when normal subjects held their breath first in "deep inspiration," compared with "deep expiration." In contrast, the changes we saw were much larger (a 77% decrease, Table I). However, those measurements were recorded after a prolonged breathhold, during the steady state when transients associated with intrathoracic pressure swings have abated. In the present study, this state is never reached because the subject breathes normally.

4) Changes in inspiratory afterload might also be thought to affect the magnitude of the BCG. During inspiration aortic transmural pressure and the impedance to left ventricular ejection increase. As a consequence stroke volume decreases (5,10,12). Thus, at end-inspiration we might expect to see a reduction in the BCG from this mechanism. However Fig. 2 shows that most of the major components of the BCG are larger at end-inspiration, which suggests that this effect is of less consequence than the increase in the coupling of the heart motion to the body at higher lung volumes.

While it is clear that lung volume has a profound influence on BCG amplitude (Fig. 2), respiratory motion itself does not. The BCG averaged at mid-inspiration is largely the same as that at mid-expiration, even though the rib cage and abdomen are moving in the opposite direction (Fig. 3). Recent observations of the BCG using a static-charge-sensitive bed have shown a strong correlation between an increased amplitude of the BCG and decreases in intrathoracic pressure (11). Our data are consistent with these observations. The similarity of the BCG at mid-inspiration (Fig. 3) and at  $FRC + V_T$  (Fig. 2) suggests that lung volume (likely through the effects of intrathoracic pressure) is the dominant effect in modulating the transmission of the forces from the heart, as opposed to respiratory motion itself.

#### *Displacement from Cardiac Motion*

Typical values of displacement along the Y-axis measured on Earth for IJ is  $-37 \mu\text{m}$  and for JK is  $+95 \mu\text{m}$  (2). Our results are consistent with those values. Fig. 4 shows the motion of the subject's body free floating in

the Spacelab during each cardiac cycle. Along the Y-axis, at  $FRC + V_T$ , in spaceflight, we recorded displacements of  $-35 \mu\text{m}$  for IJ and  $+89 \mu\text{m}$  for JK.

In the Y-axis there was a small reduction in the displacement between  $FRC + V_T$  and FRC. In contrast there were only small differences in the displacement in the X and Z axes with changes in lung volume. This is consistent with the concept that the lung acts as a more efficient shock absorber at FRC than at higher lung volumes in the Y-axis, but that the presence of rigid body structures such as the chest wall and spine result in less dependence on lung volume in the transverse axes.

#### *Respiratory Motion*

The overall acceleration of the body when the data were ensemble averaged over the respiratory cycle did not show any clear evidence of accelerations due to the cardiac cycle. This suggests that the cardiac cycle was indeed randomly timed with respect to respiration and that we had an adequate number of respiratory cycles in our average. Thus, we can be confident that the velocities and displacements shown in Fig. 5 do in fact result from respiratory motion and not from some artifact due to the heartbeat.

The overall motion of the body of the free-floating subject is consistent with previous reports of the motion of the diaphragm during breathing. Using three-dimensional reconstruction techniques, Gautier et al. (4) showed that for an approximately 2 L inspiration from FRC, the diaphragm descends  $\sim 33 \text{ mm}$ . Thus for tidal breathing, in which the volume change is likely to be  $\sim 750 \text{ ml}$ , the diaphragm descent will be  $\sim 13 \text{ mm}$ , which for a 2-s inspiration gives a velocity of  $\sim 7 \text{ mm} \cdot \text{s}^{-1}$ . The descent of the diaphragm primarily results in the movement of the upper abdominal contents in a footward direction. In a free-floating subject, conservation of momentum requires that a movement of the entire body in the opposite direction must compensate for such a motion. If we assume that the abdominal contents account for  $\sim 25\%$  of the total body mass we can calculate the expected overall body motion. While the abdominal contents are displaced downwards, the lower part is constrained by the pelvis, and so for the purposes of this discussion we will assume that the average velocity of motion is halved in the head-to-foot direction. Using these assumptions, we would predict that the footward diaphragmatic motion would be compensated for by a headward total body motion of  $\sim 0.8 \text{ mm} \cdot \text{s}^{-1}$ , with a total displacement of  $\sim 1.6 \text{ mm}$ . These approximations are comparable to the observed motions in the Y axis (Fig. 5) of  $0.6 \text{ mm} \cdot \text{s}^{-1}$  velocity and  $0.9 \text{ mm}$  displacement.

Similarly, inspiration results in an outward (ventral) movement of the anterior wall of the abdomen of  $\sim 15 \text{ mm}$  for a 2 L inspiration (4). This corresponds to a motion of  $\sim 6 \text{ mm}$  for tidal breathing. Using a similar line of reasoning, we would predict an overall dorsal movement of the body with a velocity of  $\sim 0.4 \text{ mm} \cdot \text{s}^{-1}$  and a displacement of  $\sim 0.8 \text{ mm}$ . The observed motion in the dorsal direction was  $\sim 0.5 \text{ mm} \cdot \text{s}^{-1}$  with a displacement of  $\sim 0.3 \text{ mm}$ .

Calculations of the motion of the body due to respiratory action are consistent with what would be expected based on conservation of momentum. This suggests that the system we used faithfully recorded the accelerations of the body due to both cardiac and respiratory motion. Determination of stroke volume from the BCG has been shown to be possible (9). These data suggest that the BCG may provide a useful means of non-invasively monitoring changes in stroke volume in microgravity.

#### ACKNOWLEDGMENTS

The authors acknowledge the collaboration of Fernand Colin, Pierre-Francois Migeotte and Thomas Dominique, for their scientific advice. They also thank Doris Wilke, Karl Knott, the crew of Spacelab D-2, and the DLR, ESA, and NASA personnel supporting the mission. G.K. Prisk was supported by NASA contract NAS9-17884. This work was supported by Program PRODEX (Belgium).

#### REFERENCES

1. Baevsky RM, Funtova II. Ballistocardiographic examinations of the Salyut-6, fourth expedition crewmembers. *Kosmiceskaia Biologia* 1982; 16:34-6.
2. Dock W, Mandelbaum H, Mandelbaum RA. Ballistocardiography, the application of the direct ballistocardiogram to clinical medicine. St Louis: C.V. Mosby; 1953.
3. Elzinga G, Van Den Bos GC, Knoop AA. Critical notes of ballistocardiography. Ballistocardiography and Cardiovascular Therapy. In: Proc.2nd World Congr.Ballistocard.Cardiovasc. Dynamics, Oporto, Bibl.Cardiol. Basel: Karger, 1970;(26):269-79.
4. Gauthier AP, Verbanck S, Estenne M, et al. Three-dimensional reconstruction of the in vivo human diaphragm shape at different lung volumes. *J Appl Physiol* 1994; 76:495-506.
5. Guz A, Innes JA, Murphy K. Respiratory modulation of left ventricular stroke volume in man measured using pulsed Doppler ultrasound. *J Physiol Lond* 1987; 393:499-512.
6. Hixson WC, and Beischer DE. Biotelemetry of the triaxial ballistocardiogram and electrocardiogram in a weightlessness environment. Pensacola: U.S. Navy Medical Center, 1964; Monograph No:10.
7. Krauss TP, Shure L, Little JN. Signal processing toolbox for use with MATLAB (version 4.2). Natick, MA: The Math Works, Inc., 1993; 2-136-2-137.
8. Lindqvist A, Pihlajamaki K, Jalonen J, et al. Static-charge-sensitive bed ballistocardiography in cardiovascular monitoring. *Clin Physiol* 1996; 16:23-30.
9. McKay WPS, Gregson PH, McKay BWS, Militzer J. Sternal acceleration ballistocardiography and arterial pressure wave analysis to determine stroke volume. *Clin Invest Med* 1999; 22:4-14.
10. Peters J, Kindred MK, Robotham JL. Transient analysis of cardiopulmonary interactions. II. Systolic events. *J Appl Physiol* 1988; 64:1518-26.
11. Polo O, Tafti M, Hamalainen M, et al. Respiratory variation of the ballistocardiogram during increased respiratory load and voluntary central apnoea. *Eur Respir J* 1992; 5:257-62.
12. Robotham JL, Rabson J, Permutt S, Bromberger-Barnea B. Left ventricular hemodynamics during respiration. *J Appl Physiol* 1979; 47:1295-303.
13. Scano A, Strollo M. Ballistocardiographic research in weightlessness. *Earth-Orient Applic Space Technol* 1985; 15(1.2):101-4.
14. Scarborough WR, Talbot SA. Proposals for ballistocardiographic nomenclature and conventions: revised and extended. *Circulation* 1956; 14:435-50.
15. Soames RW, Atha J. Three-dimensional ballistocardiographic responses to changes of posture. *Clin Phys Physiol Meas* 1982; 3:169-77.
16. Verbanck S, Larsson H, Linnarsson D, et al. Pulmonary tissue volume, cardiac output, and diffusing capacity in sustained microgravity. *J Appl Physiol* 1997; 83:810-6.
17. Wantier M, Estenne M, Verbanck S, et al. Chest wall mechanics in sustained microgravity. *J Appl Physiol* 1998; 84:2060-5.